

Effect of Multiple Scattering on Radiation Transmission in Absorbing-Scattering Media

W.W. Yuen* and W. Dunaway†

University of California, Santa Barbara, Santa Barbara, California

A successive approximation procedure is developed to determine the scattering correction to the Beer-Lambert law in the evaluation of the geometric mean transmittance in a general multidimensional absorbing and scattering medium. At each step of the approximation, the evaluation of an upper and lower bound of the scattering correction requires only a single integral over the volume of the scattering medium. This represents a great reduction in mathematical complexity as compared to the direct numerical approach. Results for a two-dimensional rectangular absorbing and scattering medium are presented. The procedure is shown to converge rapidly in the optically thin limit. The lower-order results are useful for engineering application to media with arbitrary optical thickness. Some interesting conclusions concerning the qualitative physical behavior of the scattering correction are also generated.

Introduction

MEASUREMENT of radiative transmission is a common experimental technique for many engineering applications. In remote sensing, transmission measurements in different atmospheric absorption windows are used to determine surface temperatures, surface emissivity, and other important geographical data.¹ In the study of thermal insulation, transmission measurements are used to determine effective radiative properties of many porous insulating materials.² In combustion, radiative transmission measurements are often used to determine flame properties. Most of the existing data reduction works assume that the transmissivity and the medium's optical thickness are related by the Beer-Lambert (B-L) law. The B-L law, however, fails for media that scatter as well as absorb radiation because the scattering process cannot be lumped together with the absorption process without a separate description. The accuracy of the conventional data reduction procedure for scattering media is thus uncertain.

In some recent works,^{3,5} the deficiency of the B-L law assumption for scattering media is recognized. But almost without exception, all of the existing works consider only infinite or semi-infinite scattering media with a parallel slab geometry. For many practical situations, in which the scattering medium is finite, the applicability of the numerical results and the solution techniques developed in these works appears doubtful. The objective of this work is to present a successive approximation procedure, based on which the scattering correction to the B-L law for media with general geometry can be estimated to within an arbitrary degree of accuracy. Only isotropic scattering is considered. Generalization of the present work to media with anisotropic scattering is quite straightforward and will be presented in future works. Specifically, successively improved estimates of the upper and lower bound of the scattering correction can be generated by the present technique with little mathematical complexity. Unlike a straightforward numerical computational approach involving multiple-variable integration, which are time con-

suming even on large main frame computers, the present approach requires only a single integration over the scattering volume for each successive approximation. For engineering applications in which a high degree of accuracy is not required for the geometric mean transmittance, the present approach is particularly convenient because the lower order results, which can be generated with little mathematical complexity, are sufficient. Numerical results for a two-dimensional rectangular scattering medium are presented to illustrate the effectiveness of the present solution approach. Based on these results, some general conclusions concerning the qualitative physical behavior of the scattering correction are generated.

Analysis

Consider the two differential areas dA_0 and dA , with an intervening absorbing-scattering medium, and the associated coordinate system and geometry as shown in Fig. 1. To illustrate the effect of scattering, the geometric-mean transmittance between dA_0 and dA can be written as

$$dF_{d_0-dA} \tau_{d_0-dA} = dF_{d_0-dA} (\tau_{d_0-dA}^0 + \tau_{d_0-dA}^S) \quad (1)$$

where dF_{d_0-dA} is the differential shape factor between dA_0 and dA , $\tau_{d_0-dA}^0$ is the transmissivity between dA_0 and dA without scattering, and $\tau_{d_0-dA}^S$ is the scattering correction. Both dA_0 and dA are assumed to be diffusely emitting and absorbing surfaces in the development of Eq. (1). The transmissivity without scattering, based on the B-L law, is given by

$$\tau_{d_0-dA}^0 = e^{-L} \quad (1a)$$

with L being the optical thickness of a line of sight between the two areas. Utilizing the same approach as developed in previous works,^{6,7} a series of successively improved estimates of the lower and upper bound of the scattering correction can be generated by some simple physical reasoning.

For example, if only the scattering correction due to single scattering is considered, a first-order estimate of the lower bound to the correction factor can be written as⁶

$$dF_{d_0-dA} \tau_{d_0-dA}^S \Big|_l = \frac{\omega}{4\pi^2} dA \int_{V_1} \frac{z_1(\vec{n} \cdot \vec{r}_1) e^{-(L_1+r_1)}}{(L_1 r_1)^3} dV_1 \quad (2)$$

The geometry for this calculation is shown in Fig. 2 with ω the scattering albedo, while

$$\vec{L}_1 = x_1 \hat{i} + y_1 \hat{j} + z_1 \hat{k} \quad (2a)$$

Presented as Paper 85-0947 at the AIAA 20th Thermophysics Conference, Williamsburg, VA, June 19-21, 1985; received Feb. 10, 1986; revision received April 24, 1986. Copyright © American Institute of Aeronautics and Astronautics, Inc., 1986. All rights reserved.

*Associate Professor, Department of Mechanical and Environmental Engineering, Member AIAA.

†Graduate Student, Department of Mechanical Engineering, Member AIAA.

and

$$\vec{r}_1 = (x-x_1)\hat{i} + (y-y_1)\hat{j} + (z-z_1)\hat{k} \quad (2b)$$

Physically Eq. (2) represents the fraction of energy that, after leaving dA_0 , is scattered once into the line-of-sight direction from dV_1 to dA . Similarly, the first-order approximation of the upper limit of the scattering correction, $[\tau_{d_1-d_2}^d]_u^1$ can be written as

$$dF_{d_0-d_A} \tau_{d_0-d_A}^d]_u^1 = \frac{\omega}{\pi} \int_{V_1} \frac{z_1 e^{-L_1}}{L_1^3} dV_1 - \int_{A_s-d_A} dF_{d_0-d_A} \tau_{d_0-d_A}^d]_i^1 \quad (3)$$

Physically, the first term in Eq. (3) represents the total amount of energy that has experienced a single scattering by the medium. The second term represents the minimum portion of that energy, which is intercepted by the boundary of the scattering volume, except dA . The difference between the two terms clearly represents an upper bound of the scattering correction to the B-L law.

The above development can be readily generalized to estimate higher-order results for the upper and lower limits of the scattering correction. In the n th order, the lower bound of $\tau_{d_0-d_A}^d$ can be written recursively in terms of the $(n-1)$ th order results as

$$dF_{d_0-d_A} \tau_{d_0-d_A}^d]_l^n = dF_{d_0-d_A} \tau_{d_0-d_A}^d]_l^{n-1} + \left(\frac{1}{\pi}\right) \left(\frac{\omega}{4\pi}\right)^n dA K_n \quad (4)$$

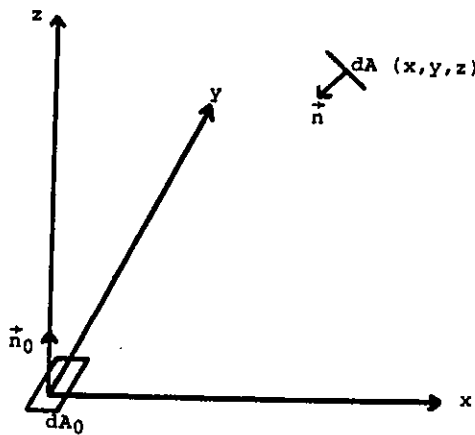


Fig. 1 Coordinate system and geometry.

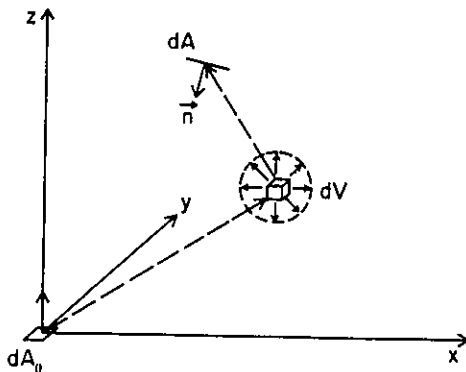


Fig. 2 Geometry for first-order calculation

where

$$K_n = \int_{V_s} \frac{(\vec{n} \cdot \vec{r}') e^{-r'}}{r'^3} J_{n-1}(V) dV \quad (5)$$

with

$$J_0 = z_1 e^{-L_1} / L_1^3 \quad (6)$$

$$J_n(V) = \int J_{n-1}(V') \frac{e^{-r'}}{r'^2} dV' \quad (6a)$$

and

$$\vec{r} = (x-x_a)\hat{i} + (y-y_a)\hat{j} + (z-z_a)\hat{k} \quad (7a)$$

$$\vec{r}' = (x-x')\hat{i} + (y+y')\hat{j} + (z-z')\hat{k} \quad (7b)$$

The subscript A denotes the coordinates of dA and the super-script prime denotes a variable of integration. The upper bound of the scattering correction is given by

$$dF_{d_0-d_A} \tau_{d_0-d_A}^d]_u^n = dF_{d_0-d_A} \tau_{d_0-d_A}^d]_l^{n-1} + \left(\frac{\omega}{\pi}\right) \left(\frac{\omega}{4\pi}\right)^{n-1} \int J_{n-1}(V) dV - \left(\frac{\omega}{\pi}\right) \left(\frac{\omega}{4\pi}\right)^n \int_{A_s-d_A} K_n dA_s \quad (8)$$

The advantage of the present technique in contrast to a straightforward numerical computation approach is apparent. At each order of the approximation, evaluations of K_n and J_n involve only a single numerical integration over the scattering medium. The integrand requires the value of J_{n-1} which is tabulated in the $(n-1)$ th approximation.

Application

As an illustration of the importance of the scattering effect and of the effectiveness of the present solution technique, the geometric-mean transmittance between an infinitesimal area dA_0 and a finite detecting area A will be calculated. In order to simplify the calculations, the medium and the detecting area will be assumed to be infinite in the y direction. The specific geometry is illustrated in Fig. 3. The geometric-mean transmittance $F_{d_0-A} \tau_{d_0-A}$ with A being both the top and side surface, will be evaluated. It is important to note that because of symmetry, the present results can also be interpreted as the radiative transfer between a finite source area A and an infinitesimal detecting area dA_0 .

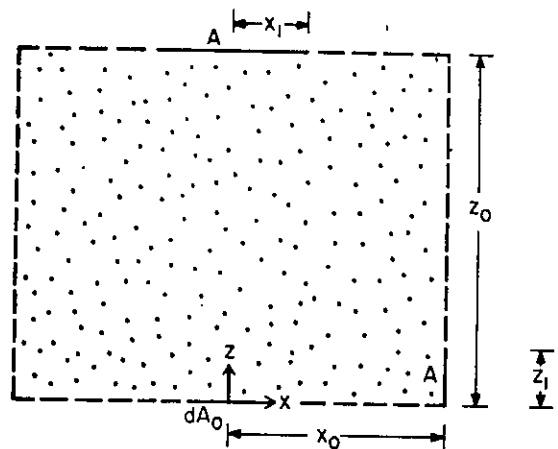


Fig. 3 Coordinate system and geometry for the two-dimensional application.

Since the medium is infinite in the y direction, Eqs. (5) and (6) may be simplified to yield

$$K_n = \pi \int \frac{(\vec{n} \cdot \vec{r}) S_n(r)}{r^2} J_{n-1}(x, z) dx dz \quad (9)$$

$$J_n(x, z) = \pi^n \int J_{n-1}(x', z') \frac{S_1(r')}{r'} dx' dz' \quad (10)$$

where

$$r = [(x_A - x)^2 + (z_A - z)^2]^{1/2} \quad (10a)$$

and

$$r' = [(x - x')^2 + (z - z')^2]^{1/2} \quad (10b)$$

Note from Fig. 3 that $z_A = z_0$ when the detecting area is at the upper surface and $x_A = x_0$ when the detecting area is at the side surface. In addition J_0 can be simplified as

$$J_0 = z S_2(L) / L^2 \quad (11a)$$

where

$$L = (x^2 + z^2)^{1/2} \quad (11b)$$

$S_1(x)$ and $S_2(x)$ are generalized exponential functions, which have been studied extensively, and their numerical values and analytical properties are presented in Ref. 8. In general, $S_n(x)$ is defined by

$$S_n(x) = \frac{1}{\pi} \int_{-\infty}^{\infty} \frac{e^{-(x^2 + y^2)^{1/2}}}{(x^2 + y^2)^{(n+1)/2}} dy \quad (12)$$

Equations (2-4) and (8), together with Eqs. (9-11), provide all of the information necessary to evaluate the scattering correction for the geometry shown in Fig. 3.

Results and Discussion

Top Surface

In analyzing the radiation transfer to the top surface, there are three interesting parameters to vary: the optical thickness of the medium (z_0), the optical width of the medium (x_0), and the optical size of the detector (x_1). These parameters are labeled in Fig. 3. To demonstrate the maximum effect of scattering of the scattering albedo, ω is taken to be 1.0 in all of the calculations.

Since the scattering contribution to the geometric-mean transmittance is being calculated, it will be useful to have available the geometric-mean transmittance without the scattering contribution, (see Eq. 1). This is given in the present example as

$$F_{d_0-d_A} T_{d_0-d_A}^0 = \int_0^{x_1} z_0^2 \frac{S_3[(x^2 + z_0^2)^{1/2}]}{(x^2 + z_0^2)^{3/2}} dx \quad (13)$$

Numerical values of this expression are plotted for various values of the detector in size x_1 in Fig. 4 for comparison with the scattering contribution, which will follow.

Since the present solution technique is an iterative process, the rate of convergence is an important consideration. This rate is shown in Fig. 5. It is immediately obvious from the figure that increasing optical thickness decreases the rate of convergence. For optically thin media, the convergence is quite rapid. For media with larger optical thickness, convergence is not achieved until higher orders are calculated.

The numerical evaluation of the upper and lower limits of the scattering correction factor was carried out to sufficiently large n to insure that the relative difference between two successive approximations was less than 0.01, except in the cases

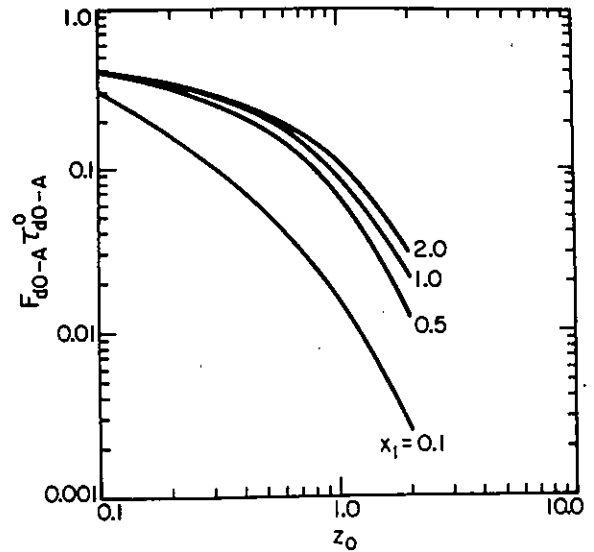


Fig. 4 Geometric-mean transmittance without the scattering contribution (top surface).

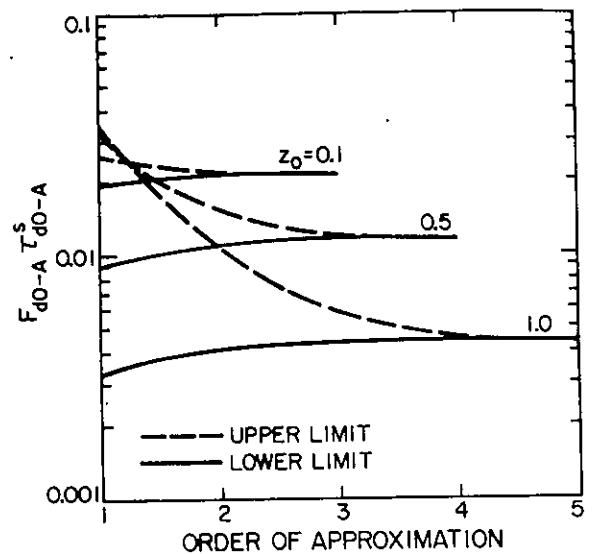


Fig. 5 Rate of convergence of the solution technique with $x_1 = x_0 = 0.1$ (top surface).

with large optical thickness ($z_0 > 1.0$), which converged slowly. In these cases, the numerical evaluation was carried out until n was approximately 9 or 10, and then a 'best estimate' of the converged value was made by considering the values of the upper and lower limits at the largest n , n_{max} , and by calculating an average weighted by the relative changes of the two limits between n_{max} and $n_{max} - 1$.

The converged values can be used to illustrate quantitatively some general conclusions about scattering media. Figure 6 shows the variation of the scattering correction factor with optical thickness for various medium widths and for a fixed detector optical size $x_1 = 0.1$. The scattering correction factor reaches a maximum value at small optical thicknesses, if the medium width is equal to the detector size, and reaches a maximum value at increasing optical thicknesses as the medium width is increased above the detector size. The magnitude of the scattering correction factor appears to become quite insensitive to medium width when the medium width is greater than the detector size, especially for small vertical optical thickness z_0 . This indicates that for an isotropically scattering medium, the contribution of the medium away from the line of sight to the scattering correction could be neglected. This conclusion

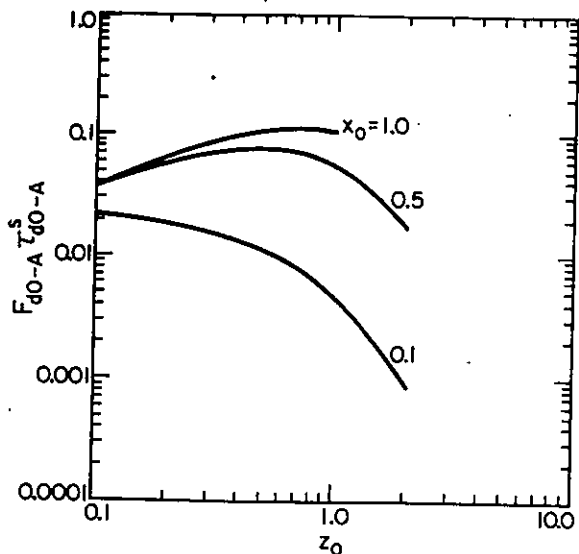


Fig. 6 Effect of the size of the scattering medium [x_0 on the scattering correction factor with $x_1 = 0.1$ (top surface)].

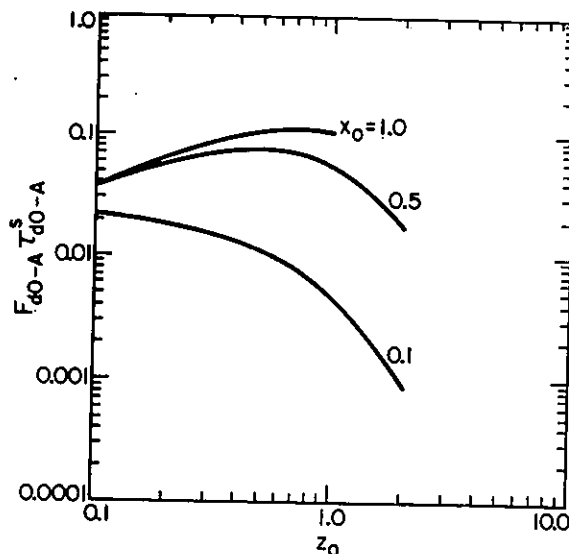


Fig. 7 The effect of optical thickness (z_0) for different x_0 with $x_1 = x_0$ (top surface).

can lead to considerable simplification of the mathematics involved in evaluating the scattering correction.

Values of the scattering correction factor are presented in Fig. 7 for different optical thicknesses and medium widths with the detector size equal to the medium width. It is interesting to compare these curves with the same information presented as a ratio of the scattering correction factor to the geometric-mean transmittance calculated without scattering, i.e.,

$$M = \frac{\tau_{d0-A}^s}{\tau_{d0-A}^0} \quad (14)$$

This ratio is plotted in Fig. 8. Figures 7 and 8 illustrate two possible interpretations of the relative importance of the scattering effect. For applications in which the magnitude of the scattering contribution is important, Fig. 7 indicates that scattering is important for systems with intermediate optical thickness, around $z_0 = 0.5$ in the present case. For systems in which the relative magnitude of the scattering contribution is important, Fig. 8 indicates that scattering increases in importance with increasing optical thickness.

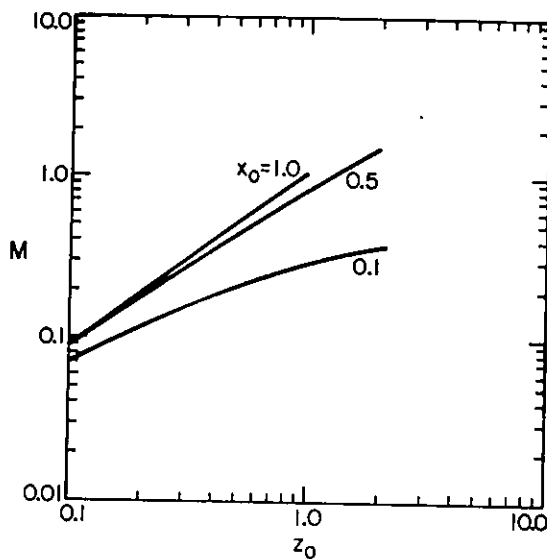


Fig. 8 Scattering factor M with $M_1 = x_0$ (top surface).

Side Surface

In the analysis of radiation transfer to the side surface, there are again three parameters to vary: the optical thickness of the medium (z_0), the optical width of the medium (x_0), and the optical size of the detector (z_1). Note from Fig. 3 that z_1 is measured from the lower corner.

The geometric-mean transmittance without the scattering contribution for this case is given by

$$F_{d0-dA} \tau_{d0-dA}^0 = \int_0^{z_1} \frac{z_1 x_0 S_3 [(x_0^2 + z^2)]^{1/2}}{(x_0^2 + z^2)^{3/2}} dz \quad (15)$$

This expression is plotted in Fig. 9 for comparison with the scattering contribution.

The rate of convergence of the process for the side surface is plotted in Fig. 10 with $z_1 = z_0 = 0.1$. It is apparent that the width of the scattering medium in this optically thin case has little effect on the rate of convergence. Figure 11 illustrates the rate of convergence for a case of larger optical thickness $z_0 = 1$. In this case, the dependence of rate of convergence on the width of the medium appears to be stronger. However, comparison of Fig. 11 with Fig. 10 shows that, as in the case of the top surface, rate of convergence depends fairly strongly on the optical thickness z_0 .

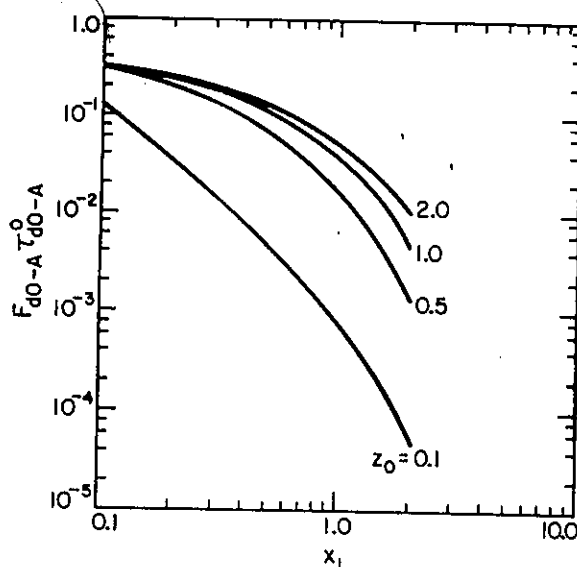


Fig. 9 Geometric-mean transmittance without the scattering contribution (side surface).

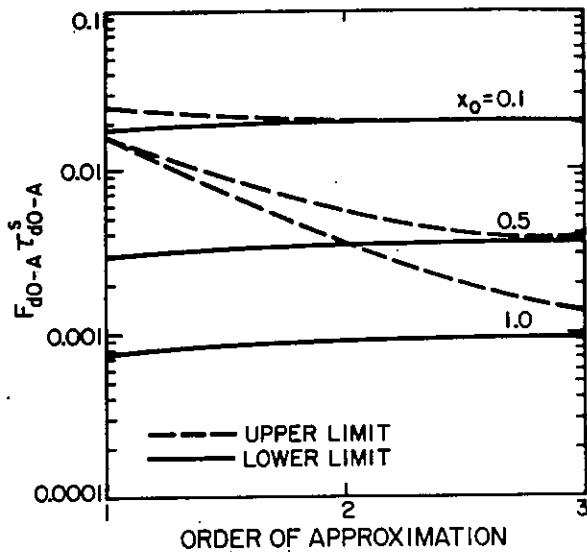


Fig. 10 Rate of convergence of the solution technique with $z_1 = z_0 = 0.1$ (side surface).

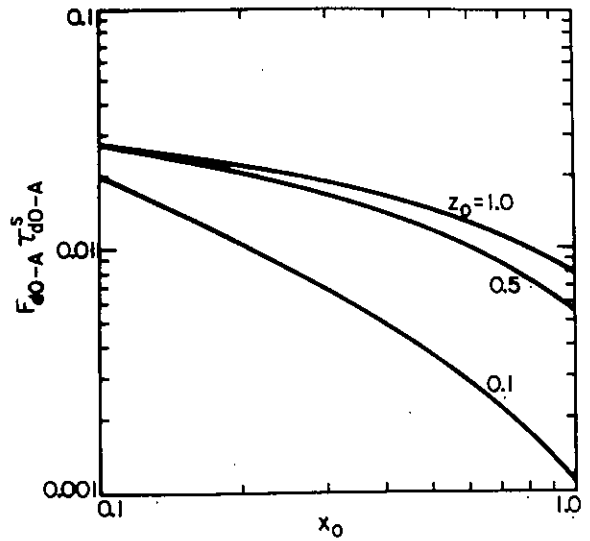


Fig. 12 Effect of optical thickness (z_0) with $z_1 = 0.1$ (side surface).

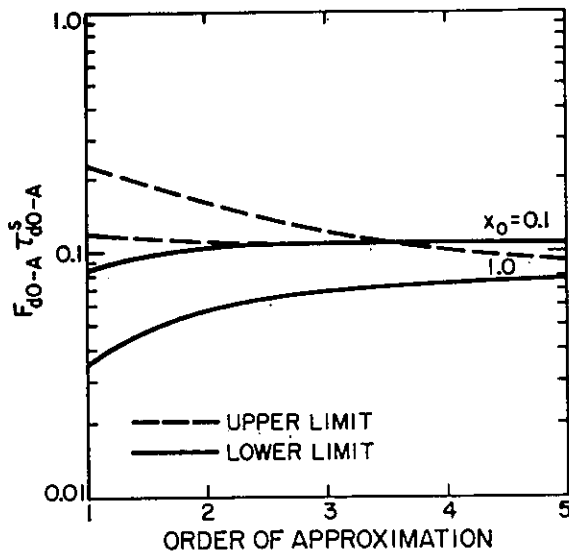


Fig. 11 Rate of convergence of the solution technique with $z_1 = z_0 = 1$ (side surface).

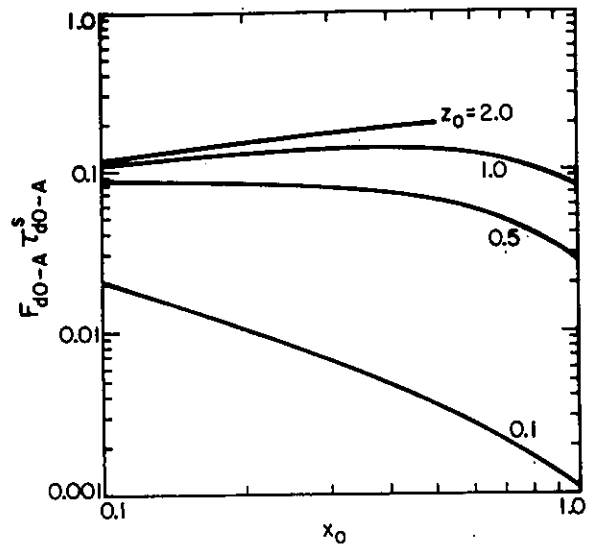


Fig. 13 The effect of z_0 and x_0 with $z_1 = z_0$ (side surface).

The magnitudes of the converged values of the scattering correction factor are plotted as a function of medium width in Fig. 12 for several values of z_0 and x_0 , with $z_1 = 0.1$. The scattering correction factor has its maximum values at small medium widths, as would be expected from physical considerations, since for large medium widths the detector is far away. The effect of z_0 decreases rapidly as z_0 becomes larger than the detector size z_1 . This suggests that, as in the top surface case, the contribution of the medium away from the line of sight could be neglected, again suggesting a possible way to reduce the mathematical complexity of the calculation.

Figure 13 shows the scattering correction factor as a function of medium width for different x_0 , with $z_1 = z_0$. As in the case of the top surface, this will be compared with the ratio of the scattering correction factor to the geometric-mean transmittance without scattering, as given by Eq. (14). This factor is plotted in Fig. 14. Figure 13 shows that the magnitude of the scattering correction factor for small z_0 decreases as the horizontal optical thickness of the scattering medium x_0 increases. For media with larger z_0 , the magnitude reaches a maximum at intermediate x_0 . This result also illustrates that for applications in which the magnitude of the scattering cor-

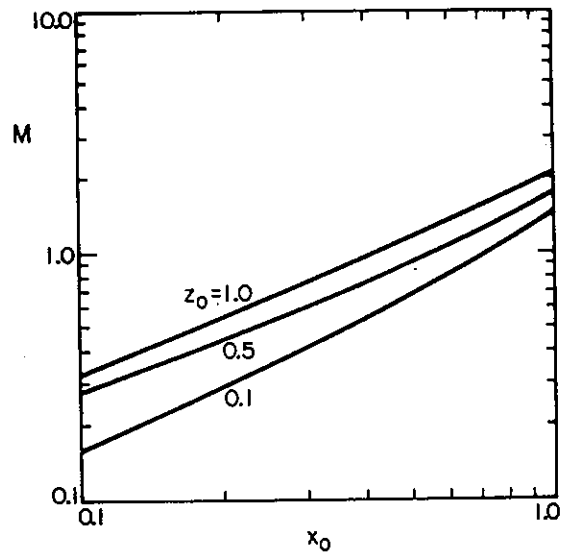


Fig. 14 Scattering factor M with $z_1 = z_0$ (side surface).

rection factor is important, the effect of scattering increases with increasing Z_0 . Figure 14 shows that for applications in which the relative value of the scattering correction factor is important, the role of scattering increases with both optical thickness z_0 and medium width x_0 .

Conclusions

A successive approximation procedure has been developed to determine the scattering correction to the geometric-mean transmittance in general multidimensional systems. At each step of the approximation, the upper and lower limits of the scattering correction can be calculated by a single integration over the volume of the scattering medium.

The application of this solution procedure to a two-dimensional rectangular scattering medium allows some interesting conclusions to be drawn concerning the physics of scattering. They are

1) For an isotropically scattering medium, the most significant contribution to the scattering correction factor comes from the medium which lies along the line of sight between the source and the detecting area.

2) In terms of the absolute magnitude of the scattering correction factor, the scattering to the top surface reaches a maximum at intermediate optical depth, while the scattering to the side surface increases with increasing optical depth. The scattering to the top surface increases as the optical width of the medium (and the size of the detector) increases. As the optical width of the scattering medium increases, the scattering to the side surface decreases if the medium is optically thin, and increases to a maximum before decreasing if the medium is optically thick.

3) In terms of the relative magnitude of the scattering correction factor (related to the geometric-mean transmittance calculated without scattering) the importance of scattering increases with optical depth and width for both the top and side surfaces.

References

- ¹Paltridge, G.W. and Platt, C.M.R., *Radiative Processes in Meteorology and Climatology*, Elsevier Scientific Publishing Co., New York, 1976.
- ²Tong, T.W. and Tien, C.L., "Radiative Heat Transfer in Fibrous Insulation—Part I: Analytical Study," *ASME Journal of Heat Transfer*, Vol. 105, Feb. 1983, pp. 70-75.
- ³Crosbie, A.L. and Koewing, J.W., "Two-Dimensional Radiative Transfer in a Finite Scattering Planar Medium," *Journal of Quantitative Spectroscopy and Radiative Transfer*, Vol. 21, June 1979, pp. 573-595.
- ⁴Tam, W.G. and Zardecki, A., "Multiple Scattering Correction to the Beer-Lambert Law. 1: Open Detector," *Applied Optics*, Vol. 21, July 1982, pp. 2405-2412.
- ⁵Tong, T.W., Liu W.L., and Subramanian, E., "The Effect of Multiple Scattering in Measuring the Radiation Properties of Absorbing and Scattering Media," AIAA Paper 83-1454, June 1983.
- ⁶Yuen, W.W., "A Limiting Approach for the Evaluation of Geometric-Mean Transmittance in a Multi-Dimensional Absorbing and Isotropically Scattering Medium," *ASME Journal of Heat Transfer*, Vol. 106, May 1984, pp. 441-447.
- ⁷Yuen, W.W. and Dunaway, W., "Calculations of the Geometric-Mean Transmittance in a Multi-Dimensional Absorbing and Anisotropically Scattering Medium," *The International Journal of Heat and Mass Transfer*, Vol. 28, No. 8, Aug. 1985, pp. 1507-1515.
- ⁸Yuen, W.W. and Wong, L.W., "The Numerical Computation of an Important Integral Function in Two-Dimensional Radiative Transfer," *The Journal of Quantitative Spectroscopy and Radiative Transfer*, Vol. 29, Feb. 1983, pp. 145-149.

From the AIAA Progress in Astronautics and Aeronautics Series...

SPACECRAFT CONTAMINATION: SOURCES AND PREVENTION — v. 91

*Edited by J.A. Roux, The University of Mississippi
and
T.D. McCay, NASA Marshall Space Flight Center*

This recent Progress Series volume treats a variety of topics dealing with spacecraft contamination and contains state-of-the-art analyses of contamination sources, contamination effects (optical and thermal), contamination measurement methods (simulated environments and orbital data), and contamination-prevention techniques. Chapters also cover causes of spacecraft contamination, and assess the particle contamination of the optical sensors during ground and launch operations of the Shuttle. The book provides both experimental and theoretical analyses (using the CONTAM computer program) of the contamination associated with the bipropellant attitude-control thrusters proposed for the Galileo spacecraft. The results are also given for particle-sampling probes in the near-field region of a solid-propellant rocket motor fired in a high-altitude ground test facility, as well as the results of the chemical composition and size distribution of potential particle contaminants.

Published in 1984, 333 pp., 6×9, illus., \$39.50 Mem., \$69.50 List; ISBN 0-915928-85-X

TO ORDER WRITE: Publications Dept., AIAA, 1633 Broadway, New York, N.Y. 10019